Noninvasive Imaging of the Distribution in Oxygen in Tissue In Vivo Using Near-Infrared Phosphors

Sergei A. Vinogradov, Leu-Wei Lo, William T. Jenkins, Sydney M. Evans, Cameron Koch, and David F. Wilson
Departments of Biochemistry and Biophysics and of Radiation Oncology, Medical School, and Department of Clinical Studies, Veterinary School, University of Pennsylvania, Philadelphia, Pennsylvania 19104 USA

ABSTRACT A newly developed water-soluble phosphor suitable for measuring oxygen pressure in the blood (Green 2W) was used for noninvasive, in vivo imaging of oxygen distribution in the vascular systems of mice. Oxygen quenches the phosphorescence of Green 2W, measured in the presence of 2% albumin, according to the Stern–Volmer relationship. This oxygen-dependent quenching of phosphorescence has been used to obtain digital maps of the oxygen distribution in the tissue vasculature. EMT-6 mammary carcinoma tumors were grown by injecting 1×10^6 cells in 0.1-ml carrier into the subcutaneous space over the muscle on the hindquarter. When the tumors were approximately 8 mm in diameter, 300 μg of phosphorescence probe (Green 2W; absorption maximum 636 nm) was injected into the tail vein. The mice were immobilized with intraperotoneal Ketamine (133 mg/kg) and Xylazine (10 mg/kg) and illuminated with flashes ($<$4-μs $t_{1/2}$) of light of 630 $\pm$ 12 nm. The emitted phosphorescence (790-nm maximum) was imaged by an intensified CCD camera. Images were collected beginning at 30, 50, 80, 120, 180, 240, 420, and 2500 μs after the flash and used to calculate digital maps of the phosphorescence lifetimes and oxygen pressure. Both the illumination light and the phosphorescence were in the near-infrared region of the spectrum, where tissue has greatly decreased absorbance. The light therefore readily passed through the skin and centimeter thicknesses of tissue. The oxygen maps could be obtained by illuminating from the side of the mouse opposite the camera (and tumor). The tumors were readily observed as regions with oxygen pressures substantially below those of the surrounding tissue. Thus, phosphorescence measurements can noninvasively detect volumes of tissue with below-normal oxygen pressure in the presence of much larger volumes of tissue with normal oxygen pressures. In addition, tissue oxygen pressures can be monitored in real time, even through centimeter thicknesses of tissue.

INTRODUCTION

Oxygen-dependent quenching of phosphorescence has been shown to be an effective method for measuring oxygen pressure and has been used to study a number of biological systems (see, for example, Robiolio et al., 1989; Wilson et al., 1988; Rumsey et al., 1990, 1991; Wilson and Cerniglia, 1992; Shonat et al., 1992a,b). Phosphorimeters in which the excitation light and phosphorescence emission were carried to and from the sample by light guides have been used to measure the oxygen dependence of respiration in in vitro suspensions of cells and mitochondria (Wilson et al., 1988; Robiolio et al., 1989; Rumsey et al., 1990) and of animal tissue in vivo including the brain cortex (Pastuszko et al., 1993; Huang et al., 1994), skin grafts on mice (Wanebo et al., 1992), and the microvasculature (Shonat et al., 1993; Torres-Filho and Intaglietta, 1993). On the other hand, a video imaging phosphorimeter has been used to obtain digital maps of oxygen distributions in tissue, including the retina of the eye (Shonat et al., 1992a,b), the cortex of the brain (Wilson et al., 1991; 1993), liver (Rumsey et al., 1988), and heart (Rumsey et al., 1994). The measurements have been limited to the surface layer of the tissue because the absorption bands of the phosphor, Pd-*meso*-tetra-(4-carboxyphenyl)-porphyrin, were all at wavelengths less than ~540 nm. At these wavelengths, absorption of the excitation light by chromophores in the tissue, notably hemoglobin, myoglobin, and cytochromes, limits the depths in tissue to which the excitation light can penetrate (and thereby phosphorescence measurements) to ~1 mm or less. The emitted phosphorescence, in contrast, has a maximum at 695 nm, where the tissue chromophores absorb much less, and can penetrate much greater thicknesses of tissue.

Recently Vinogradov and Wilson (1995) reported synthesis of a new group of oxygen-sensitive phosphors (tetrabenzoporphyrins) with absorption maxima near 636 nm and phosphorescence maxima near 800 nm. We report experiments in which a water-soluble derivative of Pd-tetrabenzoporphyrin was used to determine the oxygen distribution in the vasculature of tumor-bearing mice. These experiments establish that, by using near infrared phosphors, it is possible to image tissue oxygen distribution through centimeter thicknesses of tissue (such as through the abdomen of an adult mouse). Thus, phosphorescence quenching can now be used both to detect the presence of small regions of hypoxia (such as subcutaneous EMT-6 tumors) present in much larger volumes of normal tissue and to quantify the oxygen pressure in such hypoxic tissue volumes.

Received for publication 27 September 1995 and in final form 5 January 1996.

Address reprint requests to Dr. David F. Wilson, Room 426, Anatomy-Chemistry Building, Department of Biochemistry and Biophysics, University of Pennsylvania, Philadelphia, PA 19104. Tel.: 215-898-6383; Fax: 215-898-4217; E-mail: vinograd@mail.med.upenn.edu.

© 1996 by the Biophysical Society

0006-3495/96/04/1609/09 $2.00

MATERIALS AND METHODS

Tumor-bearing mice

Tumors were grown from cells derived from EMT-6 mammary carcinoma obtained from Dr. E. M. Lord (University of Rochester, Rochester, NY). The tumors were implanted using 1×10^6 cells suspended in 0.1-ml tissue culture medium by means of subcutaneous injection over the thigh muscle. Tumors were grown for 10–14 days until they were 0.6–0.8 cm in diameter.

Preparation of the phosphor (Green 2W), the tetrasulfonate of Pd-*meso*-tetraphenyl-tetrabenzoporphyrin

Green 2W was prepared by sulfation of the parent Pd-*meso*-tetra-(phenyl)-tetrabenzoporphyrin as previously described (Vinogradov and Wilson, 1995). The absorption spectrum and the phosphorescence spectrum of Green 2W are shown in Fig. 1. Green 2W has negligible fluorescence, and the emission is quantitatively due to phosphorescence. The quantum efficiency for phosphorescence was previously determined to be approximately 8% (Vinogradov and Wilson, 1995).

Measurements of oxygen-dependent quenching of phosphorescence in vitro

A special apparatus has been constructed to optimize calibration of oxygen-dependent quenching of phosphorescence (Lo et al., 1995). The phosphor solutions were placed in a round glass chamber with a volume of 12 ml and sealed with a top of machined ceramic. An oxygen electrode constructed of glass and ceramic (constructed in house; Koch, 1993) was fitted through a tapered hole in the top. A magnetic stirring bar sealed in ceramic and suspended from the top was used to stir the solution. The only opening into the solution was a hole (1 mm in diameter and 1.5 cm long) in the top. The sample chamber was designed such that when it was completely filled with fluid there were no gas bubbles remaining in it. The construction of glass and ceramic further limited access of oxygen to the chamber because, unlike plastics, these materials do not contain significant amounts of dissolved oxygen that could be transferred to the solution. The entire sample chamber was enclosed in an aluminum housing and surrounded by insulating foam. The phosphorescence-lifetime measurements were made through the glass wall of the chamber by use of a bifurcated light guide.

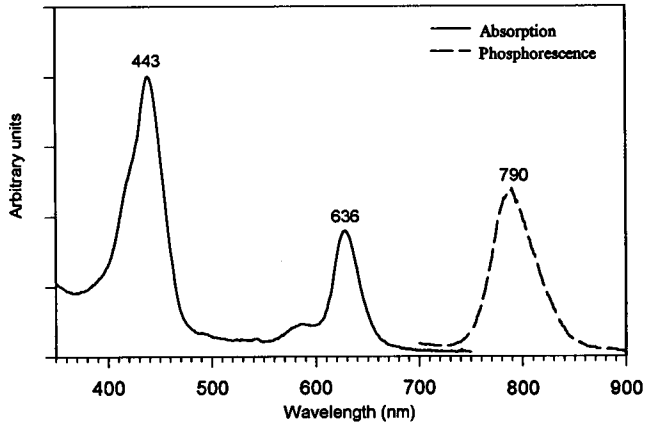

FIGURE 1 Absorption and phosphorescence emission spectra of Green 2W.

Design of the light-guide phosphorimeter

The phosphorimeter design was a modification of that of Pawlowski and Wilson (1992). Excitation light was provided by a flash lamp (45 W, 4-μs height at half-maximal intensity; EG&G Electro-Optics, Salem, MA). The light was passed through an interference filter (630 nm with a bandwidth at half-height of 23 nm) and focused on the end of a glass fiber bundle that was one half of a bifurcated light guide. The light was conducted to the common end of the light guide (a total of 6-mm-diameter bundle of fibers with a salt-and-pepper mixing), where it was focused on the sample. The emitted phosphorescence was collected by the same lens and conducted to the photomultiplier by the second half of the light guide. The phosphorescence was passed through an interference filter (820 nm with a bandwidth at half-height of 60 nm) and measured with a Hamamatsu H5527 photomultiplier cooled to -10 to -20°C in a photomultiplier housing from Products for Research, Inc. (Danvers, MA). This cooled photomultiplier was used because it has a lower noise level and greater sensitivity near 800 nm than the more usual room-temperature photomultipliers (such as the Hamamatsu R928). The photomultiplier output was amplified and digitized with a 12-bit, 1-MHz analog-to-digital board (Metrabyte Corp.; Tauton, MA, DAS 50). The digitization was started at the time the flash lamp was discharged and a total of 2024 points collected for each flash (2 ms of data). The data for multiple flashes (up to 100) were collected by summing into a 16-bit buffer. The phosphorescence-decay data were analyzed with the software developed by Pawlowski and Wilson (used for the Oxyspot phosphorimeter of Medical Systems Corp., Greenvale, NY). This software uses the least-squares technique to determine the best fit to a single exponential.

Essentially complete isolation of phosphorescence from the flash of excitation light was achieved. The phosphorescence intensity was maximal by ~6 μsec after initiation of the flash.

Imaging of phosphorescence by using Green 2W injected into the blood of mice

The mouse was anesthetized by intraperotoneal injection of Ketamine (133 mg/kg) and Xylazine (10 mg/kg), and Green 2W (0.3 mg/mouse) was injected into the tail vein. Electric hair clippers were used to remove most of the hair in the region to be measured. The mouse was then laid in a prone position on a clear plastic petri dish and illuminated with flashes of red light (630 ± 12 nm) from a flash lamp (~30 μJ of monochromatic light per flash) with a bandwidth at half-height of less than 4 μs. For experiments in which illumination was from the same side of the mouse as the camera, the light was directed onto the animal from above through a focusable ring light. For measurements through the mouse (transillumination), the excitation light was delivered through an 8-mm-diameter light guide, which directed the light upward through the bottom of the plastic petri dish.

A reference picture of the mouse was taken by reflected room light through the same camera to correlate the phosphorescence images to the superficial structures of the mouse. This picture was taken immediately preceding or immediately after the phosphorescence was imaged without altering the position of the mouse or the camera focus.

The images were taken with an intensified, red-enhanced CCD camera (Xybion) with a 60-mm zoom lens (Nikon) and an internally mounted interference filter (800 ± 30 nm). The images were digitized with an 8-bit Targa+ videographics adapter mounted in a 486 DX2–66 microcomputer (Tri-Star Computer Corp., Chandler, AZ), stored in memory, and then transferred to the hard disk. A series of phosphorescence images (512 × 480 pixels) was collected in which the camera was turned on at different times after the flash of excitation light (30, 50, 80, 120, 180, 240, 420, and 2500 μs). In each case the camera was left on for a period of 2500 μs, effectively integrating the remaining phosphorescence signal. The image-processing software then filtered (smoothed) each image with a 7 × 7 median filter, subtracted the background (image taken with a delay of 2500 μs after the flash) from each of the other images, and calculated the rate of phosphorescence decay (phosphorescence lifetime) at each pixel by best fit

to a single exponential. The digital maps of the distributions of phosphorescence lifetimes, the correlation coefficient for fit of the phosphorescence decay to a single exponential, and the phosphorescence intensity (integral of the phosphorescence output) were saved to the hard disk. The oxygen pressure at each pixel was then calculated from Eq. 1 (Stern–Volmer equation):

$$T^\circ/T = 1 + k_Q \cdot T^\circ \cdot PO_2, \quad (1)$$

where T° and T are the phosphorescence lifetimes in the absence of oxygen and in the presence of oxygen at a pressure PO_2, respectively. The second-order quenching constant k_Q and T° are experimentally determined (see below) and are characteristics of the phosphor at that temperature and pH. The digital map of oxygen pressure is then also saved to the hard disk.

RESULTS

Oxygen-dependent quenching of phosphorescence of Green 2W measured in vitro

The Green 2W was dissolved in 0.15-M NaCl at approximately 3 mg/ml, the pH adjusted to 7.4, and then the solution was diluted as required into the final solutions (from 2 to 12 μM) for measurements of the phosphorescence lifetimes as a function of oxygen pressure. As shown in Fig. 1, the excitation spectrum has two strong maxima in the visible region of the spectrum, at 450 and 636 nm, whereas the emission maximum is near 800 nm. The latter is too far into the infrared to be seen by the human eye. It should be noted that for Green 2W the excitation spectrum does not differ from the absorption spectrum, at least in the visible range. Green 2W is water soluble, but the measured values of T° and k_Q are quite variable unless albumin is added to the solution, possibly because of the formation of dimers and other soluble molecular aggregates. When albumin is added to the solution in a substantial molecular excess over the Green 2W the phosphor associates with the albumin, and access of oxygen to the phosphor is decreased, as indicated by a decrease in k_Q. The dependence of the phosphorescence quenching on the concentration of albumin in buffered saline was measured at 37°. At 0.5%, 1%, 2%, and 4% bovine serum albumin, the values for T° were 325, 330, 330, and 330 μs, respectively, and the values of k_Q were 260, 250, 255, and 250 $Torr^{-1}\ s^{-1}$, respectively. Thus the effect of albumin on the phosphorescence of Green 2W is effectively saturated by 1% albumin. Blood contains 2–4% albumin (Physiological Data Tables). The oxygen-dependent quenching of phosphorescence was therefore measured in buffered saline solutions containing 2% albumin.

The oxygen-dependent quenching of the phosphorescence of Green 2W bound to albumin is not sensitive to changes in pH within the physiological range. At pH values of 6.4, 6.8, 7.2, and 7.8 the values of T° were 325, 330, 330, and 325 μs, respectively, and the values of k_Q were 280, 250, 255, and 250 $Torr^{-1}\ s^{-1}$.

Comparison of oxygen measurements made with a high-performance oxygen electrode with those made by phosphorescence quenching

The oxygen measurements using an oxygen electrode were compared with those using phosphorescence quenching of Green 2W dissolved in buffered saline with 2% albumin as described in Materials and Methods. The oxygen pressure was measured by both the oxygen electrode and the phosphorescence lifetime of Green 2W. The oxygen pressure in the solution was lowered stepwise using ascorbate and ascorbate oxidase (Lo et al., 1995), a quantitative analysis system in which 1 mol of oxygen is stoichiometrically removed for each 2 mol of ascorbate added. The ascorbate was used as the primary standard for oxygen measurement, and the oxygen electrode as a secondary standard. There were no significant differences between the changes in oxygen measured by oxygen electrode and by phosphorescence quenching in the region from 0 to 120 Torr (Fig. 2). In the present study the tests were restricted to physiologically important pressures, which are generally less than air saturation.

Measurement of oxygen in tissue using a light guide phosphorimeter

Following intravenous injection of Green 2W, the phosphor is rapidly distributed throughout the vascular system. Bringing the common end of the light guide of the phosphorimeter to within 2 mm of the body of the mouse resulted in a strong phosphorescence from which the decay constant could be calculated. In the experiment shown in Fig. 3, the light guide was placed over the skin in the area where the

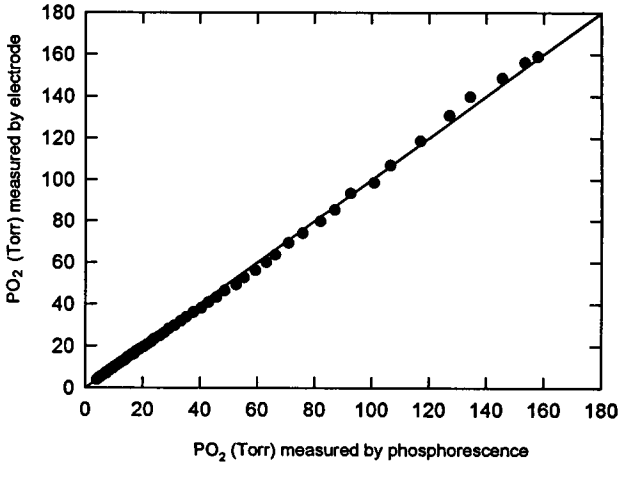

FIGURE 2 Comparison of an oxygen electrode and phosphorescence quenching in measuring oxygen in a medium. The phosphor, a Pd-*meso*-tetra-(4-carboxyphenyl) porphyrin derivative, was in solution at a concentration of 6 μM, and phosphorescence lifetime was measured through the side of the sealed glass oxygen electrode chamber. The oxygen was slowly removed by stirring the solution while passing a stream of nitrogen gas over the surface. The line at 45° is that for identical measurements by the two techniques.

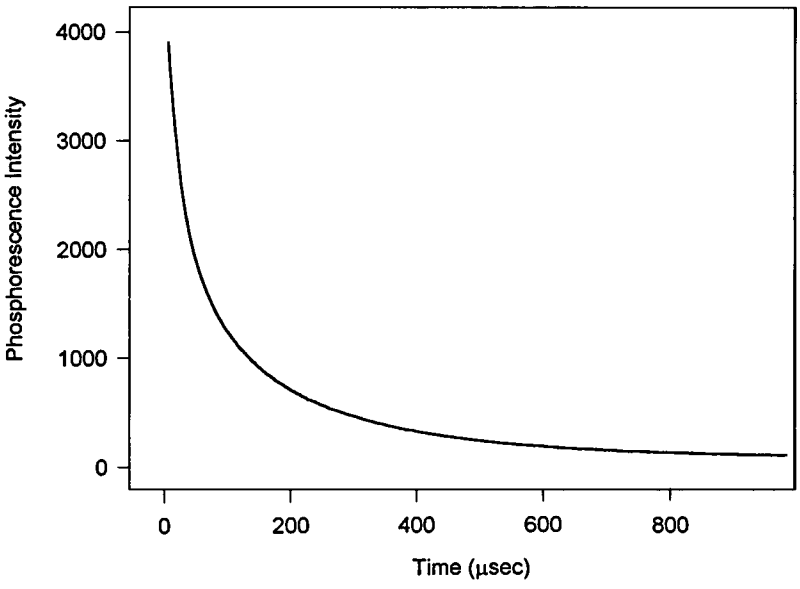

FIGURE 3 Phosphorescence signal from a mouse after i.v. injection of 0.3 mg of Green 2W. The anesthetized mouse was injected with the Green 2W through the tail vein and the phosphorescence measured with the light-guide phosphorimeter. The phosphorescence signals from 100 flashes were summed and are plotted here. The calculated S/N was ~1000.

tumor had been implanted. The phosphorescence-decay curves for a total of 100 flashes were accumulated, and the resulting signal-to-noise ratio (S/N) was approximately 1000. Measurements of the time course of changes in tissue oxygen pressure did not require such high S/N values and were usually made with an average of 10 flashes (S/N of >300) and the phosphorescence lifetime determined by best fit to a single exponential.

Further experiments were carried out in which measurements were made at 6-s intervals while the mouse was breathing air, then 95% O_2:5% CO_2 for 12 min, air again for 15 min, and finally 10% O_2:90% N_2 for 12 min (Fig. 4*A* and *B*). As the gas mixture was changed, there were rapid changes in phosphorescence lifetime and in the calculated oxygen pressure. In Fig. 4 *A* the optical field was ~5 mm in diameter and contained a small (3-mm-diameter) tumor, whereas in Fig. 4 *B* the field size was the same but the tumor was larger (~6 mm in diameter). The oxygen pressure in tissue adjacent to the tumor ranged from 30 to 40 Torr. The measured oxygen pressure for the field containing the small tumor was significantly lower, ~20 Torr. Measurements from the field with the larger tumor gave substantially lower oxygen pressures (Fig. 4 *B*).

Imaging the oxygen distribution in the tissues of mice

The phosphorescence from mice with EMT-6 tumors was imaged as described in Materials and Methods. In each case,

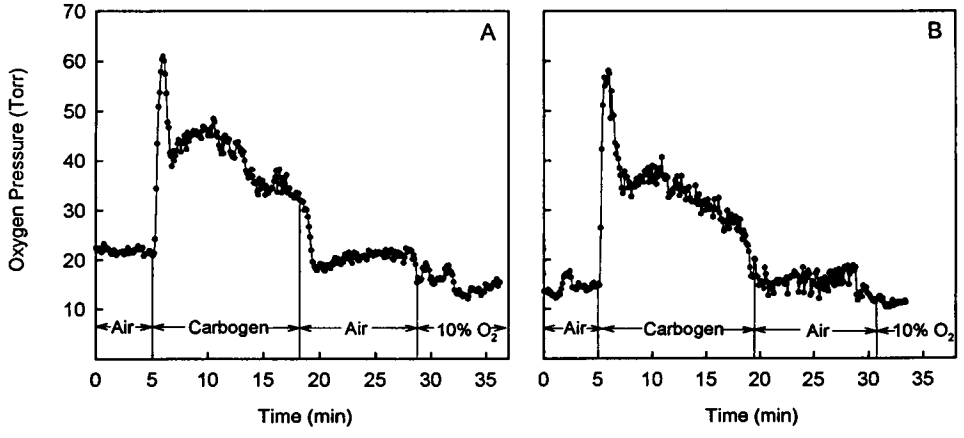

FIGURE 4 Measurements of the oxygen pressure in tumor-bearing muscle tissue of a mouse through the intact skin. Two different mice were injected with 0.3 mg of Green 2W. The common end of the light guide of a phosphorimeter (see Materials and Methods) was placed ~2 mm from the surface of the skin over the subcutaneous EMT-6 tumor, and measurements of oxygen pressure were made at 6-s intervals. After a brief control period with the mouse breathing air, the mouse was given air, 95%O_2:5% CO_2 (carbogen), air, and finally 10%O_2:90% N_2 to breathe for the time periods indicated. In *A* the tumor was ~3 mm in diameter, whereas in *B* it was ~6 mm in diameter.

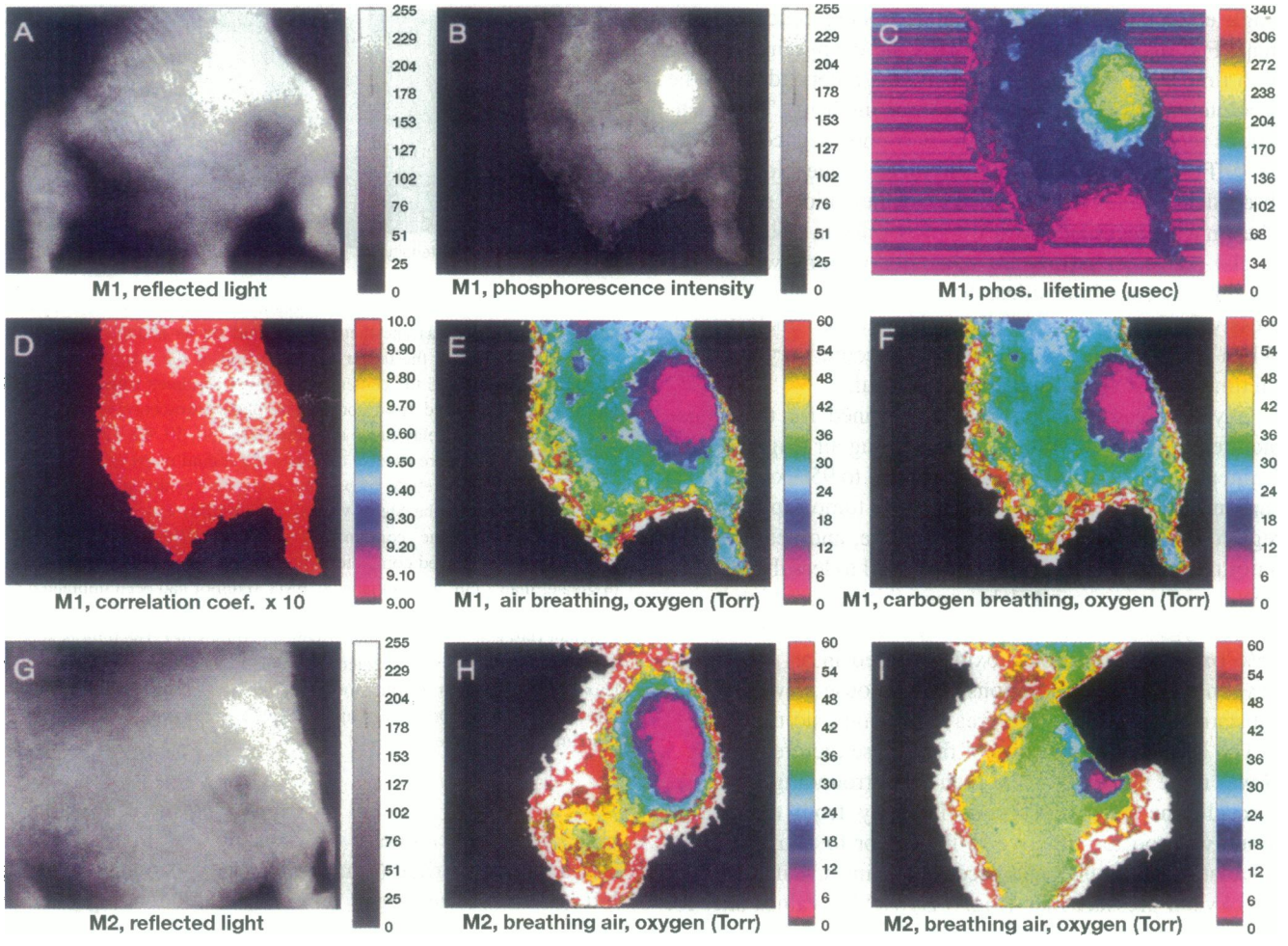

FIGURE 5 Imaging the phosphorescence of mice with subcutaneous EMT-6 tumors. The mice were imaged as described in Materials and Methods. Two different mice were anesthetized, and 0.3 mg Green 2 W was injected into the blood. Each mouse was laid on its abdomen with the tail at the top and then imaged from above with a focused ring light for illumination with the flash lamp. The first mouse was imaged by reflected room light (*A*), and then the phosphorescence was imaged with eight different delay times after the flash (30, 50, 80, 120, 180, 240, 420, and 2000 μs). The phosphorescence imaged with a delay of 30 μs is shown in Fig.6 *A* and shows that the tumor region has greater intensity than that of the surrounding tissue. The phosphorescence data set was used to calculate a map of the phosphorescence lifetimes (*C*), and the tumor area is clearly visible as a region of relatively long lifetimes (~230 μs, compared with ~100 μs). For each phosphorescence lifetime calculated there is also calculated a correlation coefficient for fit to a single exponential (*D*), and these were generally 0.99 or greater. The lifetime maps were converted to digital oxygen-pressure maps by use of the Stern–Volmer relationship and appropriate calibration constants (*E*). The tumors appear as areas of relatively low oxygen pressure, with some values less than 6 Torr. The oxygen pressure in regions of tissue removed from nontumor areas shows uniform values of 30–40 Torr. The mouse was then given carbogen (95% oxygen:5% CO_2) to breathe for 5 min, and the oxygen-pressure map was determined (*F*). The second mouse was imaged at slightly higher magnification, and the picture by room light shown in *G*. The calculated oxygen-pressure map (*H*) shows that in this mouse also the tumor appears as a region of low oxygen. The phosphorescence from the tumor was sufficiently bright, however, that it was not possible to calculate reliable phosphorescence lifetimes from the surrounding normal tissue. The tumor area was then covered with a black mask and the phosphorescence imaged again with the camera set to a higher sensitivity. The oxygen pressures are indicated in the color bars in units of Torr (dark areas correspond to low oxygen pressure). The resulting oxygen map (*I*) shows a substantial area of tissue with oxygen pressures of 35–40 Torr.

a picture of the mouse was first taken by using reflected room light (Figs. 5 *A* and *G*). This picture of the mouse can be superimposed upon the oxygen-pressure maps to correlate the measured oxygen pressures with morphological features of the mouse. An image of the phosphorescence observed with the shortest delay after the flash (30 μs) is presented in Fig. 5 *B*. The phosphorescence was not of equal intensity over the observed area of the mouse. This asymmetric distribution was the result of a combination of several different factors. Uniform illumination cannot be achieved because of the shape of the mouse, and there are heterogenous distributions of blood and oxygen pressure in the tissue (the phosphor was in solution in the blood and therefore reflected the blood volume). The tumor area has substantially greater phosphorescence intensity than its surroundings because of the combination of a higher content of blood per unit volume of tissue and lower oxygen pressure (see Fig. 5 *E*). The map of the phosphorescence lifetime calculated from the image set is shown in Fig. 5 *C*, along with the maps of the correlation coefficients for fit to a

single exponential (Fig. 5 *D*). The phosphorescence-lifetime map (Fig. 5*C*) was calculated from the change in intensity with time after the flash and as such is independent of the absolute value of the phosphorescence intensity. The calculations require, however, that the phosphorescence intensity be sufficiently large that the digitized values for at least three delay times allow reliable mathematical operations (the image processor board digitizes only in 256 intensity levels). As calculations are made for regions with lower phosphorescence intensities, the values for the lifetime progressively become noisy (poor correlation coefficients). When the phosphorescence values become very low, the lifetime values are no longer meaningful.

Oxygen-pressure maps were determined for the mouse pictured in Fig. 5 *A* while it was breathing air (Fig. 5 *E*) and 5 min after the inspired gas was changed to 95% oxygen:5% carbon dioxide (Fig. 5 *F*). The EMT-6 tumor appears as a region of below-normal oxygen pressure, and near the center of the tumor the oxygen pressures fell to less than 6 Torr. The tumor is surrounded by normal tissue, which has a mean oxygen pressure of ~35 Torr. Breathing a mixture of 95% oxygen:5% carbon dioxide resulted in an increase in oxygen pressure in all regions of the mouse as well as in a substantial decrease in the area of the hypoxic tissue.

The EMT-6 tumor region of the mouse pictured in Fig. 5 *G* was more phosphorescent than the surrounding tissue. As a result, the phosphorescence intensity from the normal tissue was too low relative to the tumor to allow accurate calculation of the phosphorescence lifetimes. Calculation of the oxygen-pressure map (Fig. 5 *H*) yielded values only for the tumor and some of the nearby tissue. The phosphorescence imaging process was repeated with a small black shield in front of the brightest region of the tumor, allowing the camera sensitivity to be increased. The increased values for the digitized phosphorescence intensities allowed calculation of the phosphorescence lifetimes for a substantial portion of the normal tissue, and the oxygen pressures were confirmed to be 35 to 40 Torr (Fig. 5 *I*).

Imaging oxygen distribution through the lower body of a mouse

Green 2W both absorbs and phosphoresces in the near infrared, allowing for maximal penetration of both excitation and emission light through tissue. As shown in Fig. 6, the oxygen distribution can easily be measured through the lower body of a mouse (~1-cm tissue thickness) including through the intact skin. This experiment was carried out in the same manner as that in Fig. 5, except that the illumination light was introduced from beneath the mouse whereas the phosphorescence was imaged from above. Diffusion of the light through the mouse resulted in a relatively uniform phosphorescence (Fig. 6 *A*), with sufficient intensity to allow good-quality images and calculation of oxygen-pressure maps. This mouse had two tumors implanted over the hindquarters. With the orientation of the mouse, the tumors were on the upper side of the mouse closest to the camera. The tumor at the right (8 mm) was larger than the one at the left (3 mm). The larger tumor is correspondingly more easily seen in the phosphorescence-lifetime and oxygen-pressure maps.

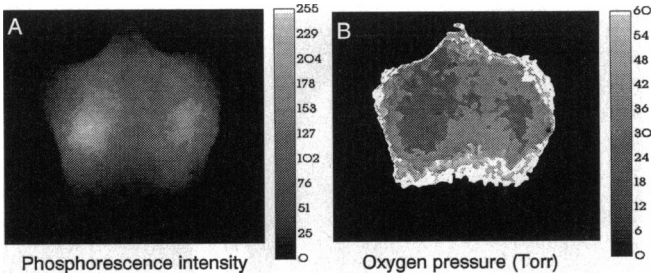

FIGURE 6 Oxygen-pressure maps obtained through the lower body of a mouse. The mouse was anesthetized and laid on its abdomen in a clear plastic petri dish with the tail at the center top of the map. The flash of excitation light entered the center of the lower abdomen from below, and the mouse was imaged from above. The phosphorescence images taken with seven different delay times after the flash (30, 50, 80, 120, 180, 240, 420, and 2000 μs) were used to calculate the digital maps of phosphorescence lifetime. The lifetime maps were converted to digital oxygen-pressure maps by use of the Stern–Volmer relationship and appropriate calibration constants. The combination of the excitation light and the phosphorescence passed completely through the mouse, a tissue thickness of greater than 1 cm. A subcutaneous EMT-6 tumor had been implanted on each flank of the mouse. These had grown to approximately 5 mm in diameter (left side) and 2–3 mm in diameter (right side). The tumors appear as areas of relatively low oxygen pressure as indicated by the gray-scale bars, with the scale from white (60 Torr) to black (0 Torr). In mice without tumors the oxygen-pressure maps are quite uniform and show oxygen pressures in the range of 30–40 Torr.

DISCUSSION

Phosphorescence quenching is an accurate measure of oxygen pressure over a wide range of PO_2 values (see, for example, Fig. 2), thus providing a particular advantage over other methods for measurement of oxygen pressures at physiological oxygen pressures and below, i.e., less than ~40 Torr (see Vanderkooi et al., 1987; Wilson et al, 1988; Lo et al., Absolute calibration of oxygen dependent quenching of phosphorescence of Pd-*meso*-tetra-(4-carboxyphenyl) porphyrin: a phosphor with general application for measuring oxygen concentration in biological systems, in preparation). The response time is only a few milliseconds, even at low oxygen pressures, and rapid measurements are possible at all oxygen pressures. These properties have made phosphorescence quenching uniquely well suited for measuring the oxygen in biological systems. As an optical method it is also very valuable in providing noninvasive, quantitative determination of the oxygen pressure in the vasculature of tissue in vivo. Phosphor dissolved in the blood can provide an excellent measure of the oxygen pressure within the microvasculature of tissue.

Some of the advantages of this method for measuring oxygen pressure in biological systems can be summarized

as follows:

1) Quenching of phosphorescence by oxygen occurs by well-understood principles, and the relationship of phosphorescence to oxygen pressure can be expressed in the form of a simple linear equation. The phosphorescence decay of the Pd-porphyrins is a single exponential, and quenching by oxygen appears to occur by a simple bimolecular collision mechanism. This means that the measured phosphorescence intensity or lifetime can be converted to oxygen pressure by using Eq. 1, where T^o is the phosphorescence lifetime in the absence of oxygen and T is the phosphorescence lifetime at oxygen pressure PO_2. The quenching constant (k_Q) is a constant related to the frequency of quenching collisions between the probe molecules in the triplet state and molecular oxygen. The value of k_Q is a function of the diffusion constants for probe and oxygen, and of temperature and probe environment. The measurements shown in Fig. 2 demonstrate that the Green 2W accurately follows Eq. 1.

2) No agents in blood, other than oxygen, affect the measured phosphorescence lifetime. The phosphor used in these experiments was bound to albumin. This means that the microenvironment of the phosphor in vivo is constant and that the calibration constants measured in vitro are valid for measurements in vivo. Moreover, once the values of k_Q and T^o have been determined for physiological conditions, they can be used indefinitely, i.e., the calibration is dependent only on the chemical structures and their microenvironment, not on the measuring apparatus or other experimental conditions. Values of k_Q and T^o determined in vitro are equally valid for measurements in vivo.

3) There is no evidence for toxicity of the Pd-porphyrins probes in current use, including Green 2W. We have injected (i.v.) 5 mg of Green 2W (~150 mg/kg) per mouse into six mice with no clinical evidence of toxicity over 10 days. With existing instrumentation, less than 0.3 mg/mouse (10 mg/kg) is sufficient for imaging the oxygen pressure, even using transillumination, and measurements with light guides require <3 mg/kg. Further increases in sensitivity and improvements in instrument design are expected to lower the Green 2W requirement for imaging to <1 mg/kg of body weight.

4) Phosphorescence lifetime is independent of probe concentration throughout the range utilized for measurements in vivo. The calibration parameters for the phosphorescent oxygen probes, such as Green 2W, bound to albumin are independent of phosphor concentration to levels well above those used for imaging and are independent of pH in the physiological range. Only the small temperature dependence (~3%/°C) need be considered.

5) Phosphorescence-lifetime measurements are independent of the absorbance or fluorescence of other chromophores that may be present in the system. Chromophores in the tissue, such as hemoglobin and myoglobin, do not substantially change absorbance during a phosphorescence decay (<1 ms) and therefore do not affect the measured phosphorescence lifetimes. Fluorophores, if present, do not interfere because measurements of phosphorescence begin a few microseconds after the flash of excitation light (and therefore fluorescence emission) has ended.

6) In samples with heterogeneous distributions of oxygen pressures, the phosphorescence-decay curves can be used to determine the distribution profile. Vinogradov and Wilson (1994) have developed an algorithm for deconvolution of the phosphorescence-decay curves from heterogenous samples to obtain the underlying distribution of phosphorescence lifetimes. Thus, it is likely that phosphorescence quenching will be able to provide histograms of the oxygen distribution in tissue.

When the phosphor is restricted to the blood, the oxygen measurements are of the oxygen pressure in the blood contained in the microvasculature. In normal tissue, with a fully developed vasculature structure, tissue hypoxia is directly related to vascular hypoxia. The capillary system is designed to provide normal tissue oxygenation when the oxygen pressure in the microvasculature is normal. It is nearly impossible to have tissue hypoxia without vascular hypoxia or vascular hypoxia without tissue hypoxia. This holds true even if there is shunting or another form of maldistribution of blood flow within the tissue. Maldistribution of flow would give rise to a mixture of hyperoxic vessels (high flow) and hypoxic (low flow) vessels, resulting in a broadened distribution of phosphorescence lifetimes. Deconvolution of the phosphorescence-decay curve would directly measure the extent of the local hypoxia resulting from the flow abnormality and therefore provide a measure of its physiological importance (see Vinogradov and Wilson, 1994).

Phosphorescence quenching has already been used to provide high-resolution digital maps of the distribution of oxygen pressure in the vasculature of a wide range of tissues in vitro (see, for example, Rumsey et al., 1988) and in vivo, including the cat eye (Shonat et al., 1992 a,b; 1993); the surface of the brain of newborn piglet (Wilson et al., 1991) and cat (Wilson et al., 1993); experimental tumors in rat (Wilson and Cerniglia, 1992); and the surface of the heart of newborn piglet (Rumsey et al., 1994). In those experiments the measurements were restricted to the surface (<0.1 mm for blue excitation, <1 mm for green excitation) of the tissue by the necessity of using visible light for excitation of the phosphor. Inasmuch as excitation light of these wavelengths is rapidly attenuated by the absorbance of other pigments in the tissue, the method was not useful for the many applications requiring tissue oxygen measurements to greater depths. The spatial resolution of measurements in thick samples is inversely related to the depth of penetration. Thus, measurements with blue light can readily attain resolution of better than 50 μm but can be made only in layers of tissue less than 100 μm thick. Near-infrared light, because of the greater thickness of tissue sampled and the correspondingly greater diffusion of the light, has a lower spatial resolution. If both phosphors are used to make measurements in thin tissue layers, however, or effective corrections are made for out-of-focus light from nearest-neighbor optical sections (pseudoconfocal microscopy), they can

provide similar spatial resolution. The theoretical limit of resolution is the same as for other optical methods, such as fluorescence imaging.

Development of the new near-infrared phosphors (Vingradov and Wilson, 1995) has made it possible to make phosphorescence measurements through substantial (centimeters) thicknesses of tissue. It is no longer necessary, for example, to remove the skin to measure oxygen pressures in the underlying muscle, making the measurements fully noninvasive. In the near-infrared region of the spectrum, tissue has a low absorbance but is highly scattering for light. The scattering process results in a rapid attenuation of the parallel component of the light beam, altering it within less than a millimeter to a nondirectional (diffuse) light that travels through the tissue in a random walk. This results in a marked increase in the light path through the tissue (see, for example, van der Zee et al., 1992). Oxygen measurements by phosphorescence quenching are not dependent on the light path of either the excitation or the emission light per se. Light scattering is, however, important in determining the thicknesses of tissue through which oxygen measurements can be made. The excitation light is attenuated as it travels through the tissue. With increasing distance from the point of light insertion the light intensity per unit volume of tissue decreases, with a proportional decrease in the efficacy of excitation of phosphorescence. The emitted phosphorescence must then diffuse through the remaining thickness of tissue to the detector. When there is equal attenuation at the wavelengths for excitation and emission, the phosphorescence-decay measurement is equally sensitive to the oxygen pressure in the blood at all positions through the thickness of the tissue between the excitation source and the detector. When the tissue has different transmission coefficients for the excitation and the emission light, the oxygen measurements will be weighted toward the side for which the light is most rapidly attenuated. If the excitation light is more strongly attenuated than the phosphorescence, for example, the oxygen measurements will be weighted toward the tissue where the excitation light enters.

Green 2W has a strong absorption at 636 nm (with an extinction coefficient of $\sim 51\ mM^{-1}\ cm^{-1}$), providing excellent efficiency for excitation of phosphorescence. This strong absorption plus the quantum efficiency for phosphorescence of ~8% (Vingradov and Wilson, 1995) results in a high phosphorescence intensity. This minimizes the technical requirements for the phosphorescence measurements and improves the quality of the resulting digital maps. In the present experiments, it was demonstrated that images of phosphorescence could already be obtained through the lower body of a mouse, or through at least 1 cm of tissue. The oxygen levels observed in the EMT-6 tumors correspond to those obtained by using 2-nitroimidazole binding and inferred from their response to radiation (Evans and Koch, unpublished results). It is reasonable to suggest that by optimizing the measurements, including the use of higher-intensity excitation light, the measurements can be extended to tissue thicknesses of 5 cm or greater. The excitation light used (<30 μJ/flash) can be increased 10- to 100-fold with a corresponding increase in phosphorescence intensity, and intensified CCD cameras are available with 10-fold greater sensitivity than that used in our study. Similarly, programs in which multiple images can be summed to provide more than 8 bits of information (such as summing into 16-bit buffers) will improve the ability to calculate oxygen-pressure maps for regions of tissues with great differences in phosphorescence intensity.

An even larger increase in sensitivity can be attained by use of point measurements instead of the CCD array for phosphorescence measurement. Point measurements made with a light guide can be at least 10^5 times more sensitive than imaging because the light can be measured with a single detector, compared with the 256,000 pixels (detectors) in the CCD array of the video camera. These considerations indicate that, although oxygen measurements in tissue using phosphorescence quenching are already providing excellent results, technical improvements over the next few years will continue to improve the quality in the resulting data and range of applicability of the method.

This research was supported in part by grants CA56679 and NS-31465 from the U.S. National Institutes of Health.

REFERENCES

Huang, Ch-Ch., N. S. Lajevadi, O. Tammela, A. Pastuszko, M. Delivoria-Papadopoulos, and D. F. Wilson. 1994. Relationship of extracellular dopamine in striatum of newborn piglets to cortical oxygen pressure. *Neurochem. Res.* 19:640–655.

Koch, C. K. 1993. Polarographic oxygen sensor. Canadian patent 1320249, 13 July.

Pastuszko, A., N, S. Lajevardi, J. Chen, O. Tammela, D. F. Wilson, and M. Delivoria-Papadopoulos. 1993. The effects of graded levels of tissue oxygen pressure on dopamine metabolism in the striatum of newborn piglets. *J. Neurochem.* 60:161–166.

Pawlowski, M., and D. F. Wilson. 1992. Monitoring of the oxygen pressure in the blood of live animals using the oxygen dependent quenching of phosphorescence. *Adv. Exp. Med. Biol.* 316:179–185.

Robiolio, M., W. L. Rumsey, and D. F. Wilson. 1989. Oxygen diffusion and mitochondrial respiration in neuroblastoma cells. *Am. J. Physiol.* 256:C1207-C1213.

Rumsey, W. L., R. Iturriaga, D. Spergel, S. Lahiri, and D. F. Wilson. 1991. Optical measurements of the dependence of chemoreception on oxygen pressure in the cat carotid body. *Am. J. Physiol.* 261: C614-C622.

Rumsey, W. L., M. Pawlowski, N. Lejavardi, and D. F. Wilson. 1994. Oxygen pressure distribution in the heart in vivo and evaluation of the ischemic "border zone." *Am. J. Physiol.* 266:H1676–1680.

Rumsey, W. L., C. Schlosser, E. M. Nuutinen, M. Robiolo, and D. F. Wilson. 1990. Cellular energetics and the oxygen dependence of respiration in cardiac myocytes isolated from adult rat. *J. Biol. Chem.* 265:15392–15399.

Rumsey, W. L., J. M. Vanderkooi, and D. F. Wilson. 1988. Imaging of phosphorescence: a novel method for measuring the distribution of oxygen in perfused tissue. *Science.* 241:1649–1651.

Shonat, R. D., A. Toth, and P. C. Johnson. 1993. Local oxygen tension measurements in the microvasculature using a new phosphorescence lifetime technique. *FASEB J.* 7:A902.

Shonat, R. D., D. F. Wilson, C. E. Riva, and S. D. Cranston. 1992a. Effect of acute increases in intraocular pressure on intravascular optic nerve

head oxygen tension in cats. *Invest. Ophthalmol. Vis. Sci.* 33: 3174–3180.

Shonat, R. D., D. F. Wilson, C. E. Riva, and M. Pawlowski. 1992b. Oxygen distribution in the retinal and choroidal vessels of the cat as measured by a new phosphorescence imaging method. *Appl. Opt.* 33:3711–3718.

Torres-Filho, I. P., and M. Intaglietta. 1993. Microvessel pO_2 measurements by phosphorescence decay method. *Am. J. Physiol.* 265:H1434- H1438.

van der Zee, P., M. Cope, S. R. Arridge, L.A. Essenpreis, A. D. Potter, J. S. Edwards, J. S. Wyatt, D. C. McCormick, S. C. Roth, E. O. R. Reynolds, and D. T. Delpy. 1992. Experimentally measured optical pathlengths for the adult heart, calf, and forearm and the head of the newborn infant as a function of inter optode spacing. *Adv. Exp. Med. Biol.* 316:143–153.

Vanderkooi, J. M., G. Maniara, T. J. Green, and D. F. Wilson. 1987. An optical method for measurement of dioxygen concentration based on quenching of phosphorescence. *J. Biol. Chem.* 262:5476–5482.

Vinogradov, S. A., and D. F. Wilson. 1994. Phosphorescence lifetime analysis with a quadratic programming algorthm for determining quencher distributions in heterogenous systems. *Biophys. J.* 67: 2048–2059.

Vinogradov, S. A., and D. F. Wilson. 1995. Metallotetrabenzoporphyrins. New phosphorescent probes for oxygen measurements. *J. Chem. Soc. Perkin Trans. II*, 103–111.

Wanebo, J., L. Weismann, L. McKinney, and F. Pierce. 1992. Long term (7 day), non-invasive monitoring of skin flap pO_2 using oxygen quenched phosphorescence decay measurements. *FASEB J.* 6:A1059.

Wilson, D. F., W. L. Rumsey, T. J. Green, and J. M. Vanderkooi. 1988. The oxygen dependence of mitochondrial oxidative phosphorylation measured by a new optical method for measuring oxygen. *J. Biol. Chem.* 263:2712–2718.

Wilson, D. F., A. Pastuszko, J. E. DiGiacomo, M. Pawlowski, R. Schneiderman, and M. Delivoria-Papadopoulos. 1991. Effect of hyperventilation on oxygenation of the brain cortex of newborn piglets. *J. Appl. Physiol.* 70:2691–2696.

Wilson, D. F., and G. J. Cerniglia. 1992. Localization of tumors and evaluation of their state of oxygenation by phosphorescence imaging. *Cancer Res.* 52:3988–3993.

Wilson, D. F., S. Gomi, A. Pastuszko, and J. H. Greenberg. 1993. Microvascular damage in the cortex of the cat from middle cerebral artery occlusion and reperfusion. *J. Appl. Physiol.* 74:580–589.